NUMERICAL MODELLING FOR SHEAR STRENGTH EVALUATION OF A HIGH PERFORMANCE FIBRE REINFORCED CONCRETE BEAM ACCORDING TO FIB MODEL CODE 2010 GUIDELINES

Rodolfo Giacomim Mendes de Andrade

rodolfogma@coc.ufrj.br

Magno Teixeira Mota

magnomota@coc.ufrj.br

Michèle Schubert Pfeil

mpfeil@coc.ufrj.br

Romildo Dias Toledo Filho

toledo@coc.ufrj.br

Ronaldo Carvalho Battista

controllato1@gmail.com

Eduardo de Moraes Rego Fairbairn

eduardo@coc.ufrj.br

COPPE – Universidade Federal do Rio de Janeiro

Av. Horácio Macedo, 2030, Centro de Tecnologia – NUMATS – Bloco I – Sala 110, CEP 21941-972, Rio de Janeiro, RJ, Brazil.

Abstract. *For scenarios where a structure is more susceptible to fail in shear instead of bending and presents a high ratio of transverse reinforcement, dispersed steel fibre reinforcement is found to contribute not only to shear strength but to post-cracking behaviour. A proposed cross-section of a High Performance Fibre Reinforced Concrete (HPFRC) beam fits this scenario due to its slender web thickness. The evaluation of the design shear strength can be performed by either analytical procedures or numerical procedures via nonlinear finite element analyses. The new fib Model Code 2010 presents a calculation method divided into four levels of approximation - levels I to III, to be performed by analytical procedures, and level IV, by numerical procedures - whereas their complexity rises with the calculation accuracy, as well as shear strength. This paper describes the calculations of all four levels of approximation, especially the fourth, in which nonlinear finite element analyses were aided by DIANA FEA BV software. As expected, for the proposed cross-section a gradual increase in shear strength*

Proceedings of the XXXVIII Iberian Latin-American Congress on Computational Methods in Engineering
P.O. Faria, R.H. Lopez, L.F.F. Miguel, W.J.S. Gomes, M. Noronha (Editores), ABMEC, Florianópolis, SC, Brazil, November 5-8, 2017.

capacity was observed for each Level of Approximation, emphasizing that the simplest level can be very conservative whilst the last can provide considerably higher strength values when compared to analytical methods.

Keywords: *HPFRC, Shear Strength, Nonlinear finite element analysis.*

1 INTRODUCTION

When designing structural fibre reinforced cementitious composite elements, the ultimate strength strongly depends on two concomitant parameters: (1) post-cracking behaviour due to fibre orientation that yields to a constitutive equation, and (2) element thicknesses, in which for each chosen dimension a different fibre orientation and dispersion can be obtained, hence affecting post-cracking behaviour.

Thus, this paper presents calculation procedures to obtain the ultimate shear strength according to *fib* Model Code 2010 (fib, 2012) recommendations taking into account a yet unknown fibre distribution. From these procedures, it is expected that a reliable shear strength is obtained from a given web thickness.

This paper is structured as follows. Item 2 describes the concepts of high performance fibre reinforced concrete and its drawback regarding fibre distribution and orientation. Then, Item 3 presents shear design according to *fib* Model Code 2010 (fib, 2012) for reinforced and high performance fibre reinforced concretes. Item 4 contains the analytical calculations and nonlinear finite element analyses for shear strength evaluation. Finally, Item 5 outlines the conclusions of this paper.

2 HIGH PERFORMANCE FIBRE REINFORCED CONCRETE

For the past decades, the addition of steel fibres in cementitious composites are considerably increasing. From FRC to HPFRC and more recently to UHPFRC, these types of materials have been structurally applied in many engineering fields, such as bridges, rehabilitation and strengthening of damaged structures, nuclear waste container, etc (Sorelli et al, 2007). However, due to its length and dispersion inside the cementitious matrix, steel fibres orientation is strongly influenced by the method of casting (Walraven, 2009). Hence, predicting fibre distribution and their effective contribution to the post-cracking behaviour of the material is a cumbersome task and some procedures to mitigate this drawback are required.

2.1 Influence of Fibre Distribution

The influence of fibre distribution and consequently its mechanical behaviour can be directly observed when performing flexural tensile strength tests (usually 3- or 4-point flexural tests). A test performed by Svec et al (2014) consisted in casting a thick slab from a specific and steady place (black arrow illustrated in Figure 1-a). From the sawed prisms extracted, 3-point flexural tests were performed and a wide range of flexural stresses were observed (Figure 1-b). The flexural behaviour of the prisms varied from deflection softening to deflection hardening, showing that extracted specimens from the same structural element can present different post-cracking behaviours, which directly interfere in flexural, shear and torsional strengths, as well as durability.

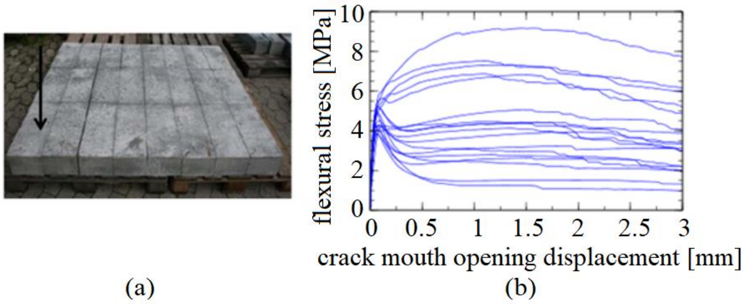

Figure 1. Experimental investigation of fibre distribution: (a) sawed slab and (b) range of structural behaviour of sawed specimens under 3-Point bending test (Svec et al, 2014)

The aforementioned range of strengths can be explained from Figure 2, where it is shown that the inclination of the fracture plane (and hence the number of fibres crossing this plane) influences the material's tensile strength.

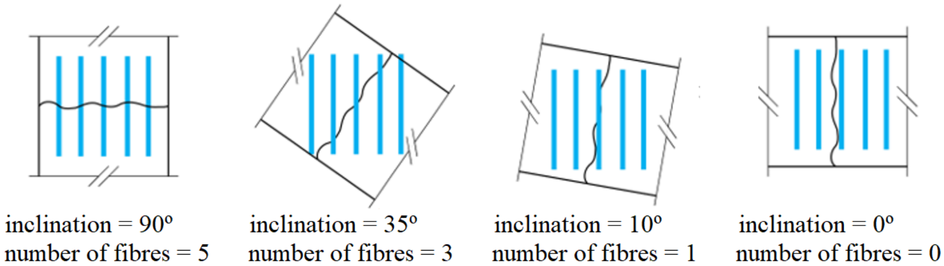

Figure 2. Steel fibres contribution to tensile strength at four different fracture planes (adapted from SFRC - Consortium, 2013)

2.2 Fibre distribution factor via mock-ups

AFGC/SETRA (2013) recommend the construction of a representative mock-up not only to define a proper method of casting and consequently obtain an improved fibre orientation, but to validate the requirements for the structural element, such as curing, casting of areas with dense reinforcement and concrete cover tolerance. An example of a mock-up with proposed specimens to be extracted can be seen in Figure 3. Each extracted specimen will be submitted to a flexural test so every critical region can have their own constitutive equation.

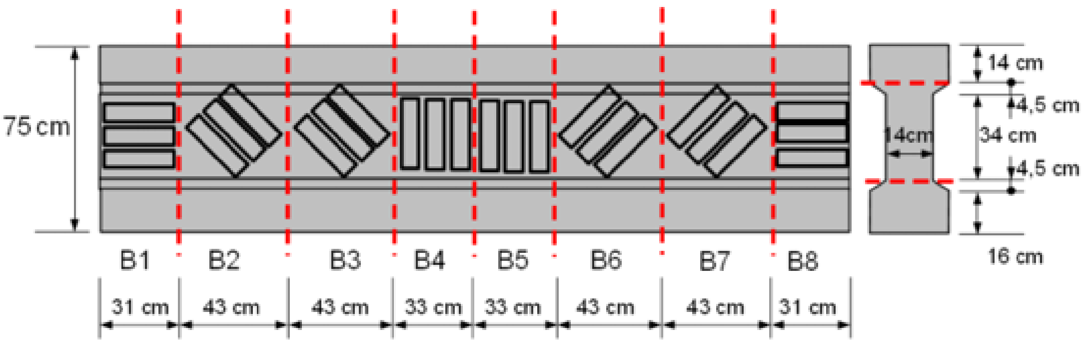

Figure 3. Mock-up specimens extraction through sawing (AFGC/SETRA, 2013)

Thus, for any given structural element geometry which has not been taken into account the fully understanding of fibre orientation, it is strongly recommended that a mock-up be constructed and sawed prisms be extracted from the most critical areas, usually determined from a preliminary elastic analysis of a numerical model.

3 SHEAR DESIGN ACCORDING TO FIB MODEL CODE 2010

3.1 Reinforced Concrete Beams with Shear Reinforcement

Whilst main codes such as fib Model Code 1990, Eurocode 2 and ACI 318 provide empirical relations for shear design, fib Model Code 2010 offers a novel approach based on physical models and important influences (e.g. strain dependence of material's strength) (Sigrist & Hackbarth, 2012).

fib Model Code 2010 (fib, 2012) proposes different shear design methods which yields to four different levels of approximation. As each level is taken, there is an increase in complexity and accuracy of the calculation procedures (Fig. 4). The first three levels are based on analytical solutions whilst the fourth level of approximation is based on nonlinear finite element analysis. The parameters that distinguish Levels I to III are the inclination of the compressive stress field in the web of a beam, θ, and the factor k_v that takes into account the concrete contribution to shear strength.

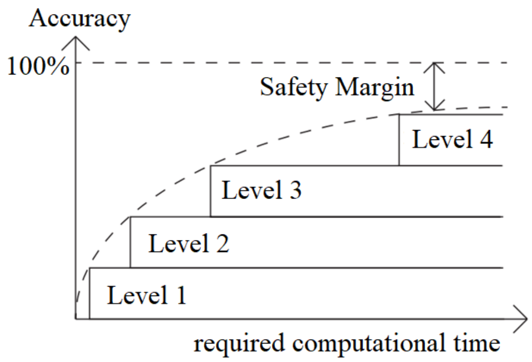

Figure 4 Accuracy versus computational time for each LoA (Lantsoght et. Al, 2016)

The Level of Approximation I is the simplest level compared to the other three. It is recommended when design procedures are found in preliminary stages and low computational effort is required (Sigrist et al, 2013). This level is a simplified version of Level III, both being based on the Modified Compression Field Theory, proposed by Vecchio and Collins in 1986. The second Level of Approximation is based on the principles of plasticity modified with a strain term to better model the behaviour of heavily reinforced members. As in Level I, Level II disregards concrete contribution to shear strength (Bentz, 2010). On the other hand, the structural design according to Level of Approximation IV is to be performed by nonlinear analysis under three possible safety formats: the Global Resistance Factor method (GRF), the Partial Factor method (PF) and the Estimation of Coefficient of Variation of Resistance method (ECOV) (Belletti et al, 2013). However, this paper will focus only in comparing the four methods without considering any safety factors – only characteristic values will be taken into account.

fib Model Code 2010 (fib, 2012) provides for shear strength of reinforced concrete the following equation:

$$V_{Rd} = V_{Rd,c} + V_{Rd,s} \geq V_{Ed} \tag{1}$$

where:

V_{Ed} is the design shear force

V_{Rd} is the design shear resistance

$V_{Rd,c}$ is the design shear resistance attributed to the concrete, given by Eq. 2

$$V_{Rd,c} = k_v \cdot \frac{\sqrt{f_{ck}}}{\gamma_c} \cdot b_w \cdot z \tag{2}$$

$V_{Rd,s}$ is the design shear resistance provided by shear reinforcement, given by Eq. 3 for vertical stirrups only:

$$V_{Rd,s} = \frac{A_{sw}}{s} \cdot z \cdot f_{ywd} \cdot cot\theta \tag{3}$$

where:

A_{sw} is the area of shear reinforcement

s is the longitudinal spacing between adjacent stirrups

f_{ywd} is the design yield strength of the shear reinforcement

z is the internal lever arm between the flexural tensile and compressive forces, as shown in Fig. 5

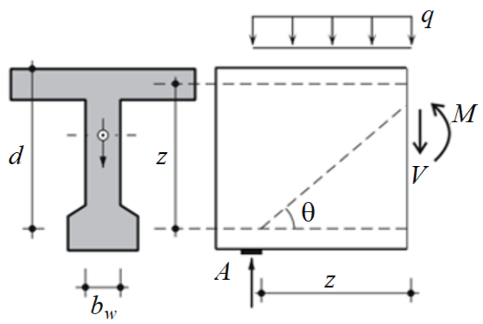

Figure 5. Internal lever arm, z (Sigrist & Hackbarth, 2010)

Also, design shear resistance must be in compliance with the following condition:

$$V_{Rd} \leq V_{Rd,max}(\theta) \tag{4}$$

where:

$$V_{Rd,max}(\theta) = k_c \cdot \frac{f_{ck}}{\gamma_c} \cdot b_w \cdot z \cdot sin\theta \cdot cos\theta \tag{5}$$

being:

$$k_c = k_\varepsilon \cdot \eta_{fc} \tag{6}$$

where:

k_ε is a factor to consider the state of strain in the web of beams

η_{fc} is a factor to take into account more brittle failure of concrete with greater strength

Although fib Model Code 2010 (fib, 2012) provides information for shear design of structural elements with and without transverse reinforcement, this paper only takes into account the equations that consider the presence of stirrups. Therefore, all structural elements must present at least a minimum reinforcement ratio of:

$$\rho_w = \frac{A_{sw}}{b_w \cdot s_w} \geq 0.08 \cdot \frac{\sqrt{f_{ck}}}{f_{yk}} \tag{7}$$

3.2 Level of Approximation I

Unlike Eq. 1, shear design according to the Level of Approximation I only takes into account the contribution of steel reinforcement, being:

$$V_{Rd} = V_{Rd,s} \geq V_{Ed} \tag{8}$$

In order to design an element according to the Level of Approximation I, the following criteria must be followed:

- For reinforced concrete elements, the minimum inclination of the compressive stress field must be $\theta_{min} = 30°$, whilst $\theta_{min} = 25°$ for prestressed elements;
- The width of the beam or web shall be checked for the selected inclinations of the compression stresses where $k_\varepsilon = 0.55$;
- Equations attributed to LoA I, are only applied when $\varepsilon_x \leq 0.001$
- ε_x is the longitudinal strain at mid-depth of shear depth and can be obtained from the following equation, applied to reinforced concrete beam subjected to simple bending:

$$\varepsilon_x = \frac{\frac{M_{Ed}}{z} + V_{Ed}}{2 \cdot (E_s \cdot A_s)} \tag{9}$$

where:

M_{Ed} is the design bending moment

V_{Ed} is the design shear force

E_s is the modulus of elasticity of reinforcing steel

A_s is the main longitudinal reinforcing bars in the tensile chord

3.3 Level of Approximation II

For this method, as considered in previous level, no concrete contribution is included in shear design strength (Eq. 1), but the angle of principal compression varies and can be selected within the proposed range:

$$20° + 10{,}000 \cdot \varepsilon_x \leq \theta \leq 45° \tag{10}$$

For mid-depth strain a value of $\varepsilon_x = 0.001$ is recommended in case of preliminary design or analysis.

Opposed to the constant value for $\boldsymbol{k_\varepsilon}$ as in Level of Approximation I, here it is taken as:

$$k_\varepsilon = \frac{1}{1.2 + 55 \cdot \varepsilon_1} \leq 0.65 \tag{11}$$

where:

$$\varepsilon_1 = \varepsilon_x + (\varepsilon_x + 0.002) \cdot cot^2\theta \tag{12}$$

3.4 Level of Approximation III

The third and last analytical level is the only one which takes into account the contribution of concrete, $V_{Rd,c}$. For the design shear resistance attributed to the concrete, the following equation shall be used:

$$k_v = \frac{0.4}{1 + 1500 \cdot \varepsilon_x} \cdot \left(1 - \frac{V_{Ed}}{V_{Rd,max}(\theta_{min})}\right) \tag{13}$$

When $V_{Rd} \geq V_{Rd,max}(\theta_{min})$, the resistance is determined as in the Level of Approximation II.

3.5 Level of Approximation IV

Although the use of Finite Element Method softwares as a tool for designing reinforced and fibre-reinforced concrete structures has been increasing, building codes do not provide detailed information on how to perform these analyses (Belletti et al, 2013).

Model Code 2010`s Level of Approximation IV requires that a design model is created according to Nonlinear Finite Element Analysis (NLFEA) criteria, providing three safety formats:

- Global Resistance Factor (GRF);
- Partial Factor (PF);
- Estimation of Coefficient of Variation of resistance (ECOV).

As previously explained, this paper will not focus on the design criteria above, attaining only to the development of Nonlinear Finite Element models without any partial safety factors.

3.6 Contribution of Steel Fibres

When considering the addition of steel fibres, fib Model Code 2010 (fib, 2012) offers two approaches to satisfy the design condition. Then, Eq. 1 becomes:

$$V_{Rd} = V_{Rd,f} + V_{Rd,s} \geq V_{Ed} \tag{14}$$

where:

V_{Rf} is the design shear resistance attributed to the concrete and the steel fibres

The first approach, which is given by the following equation, will not be considered in this paper:

$$V_{Rd,f} = \left\{ \frac{0.18}{\gamma_c} \cdot k \cdot \left[100 \cdot \rho_l \cdot \left(1 + 7.5 \cdot \frac{f_{Ftuk}}{f_{ctk}} \right) \cdot f_{ck} \right]^{\frac{1}{3}} + 0.15 \cdot \sigma_{cp} \right\} \cdot b_w \cdot d \tag{15}$$

Approach 2, to be considered in this paper due to its relation to the Levels of Approximation, is given by the following equation:

$$V_{Rd,f} = \frac{1}{\gamma_F} \cdot \left(k_v \cdot \sqrt{f_{ck}} + k_f \cdot f_{Ftuk} \cdot cot\theta \right) \cdot z \cdot b_w \tag{16}$$

where:

f_{Ftuk} is characteristic value of the ultimate tensile strength for FRC, as determined by direct tensile tests, taken at the crack width at ultimate, w_u.

$k_f = 0.8$

$$k_v = \frac{0.4}{1 + 1500 \cdot \varepsilon_x} \quad \text{, when in presence of reinforcement ratio} \tag{17}$$

Also, the limits of the angle of the compressive stress field must satisfy $\theta_{min} \leq \theta \leq 45°$, where:

$$\theta_{min} = 29° + 7000 \cdot \varepsilon_x \tag{18}$$

The value of f_{Ftuk} is determined upon consideration of:

$$w_u = 0.2 + 1000 \cdot \varepsilon_x \geq 0.125mm \tag{19}$$

4 TESTS AND SIMULATIONS

Considering the sensitivity of fibre orientation on post-cracking behaviour, a mock-up is to be built in order to verify the proposed constitutive equation to concrete tensile strength and suggest the casting pattern so the highest shear strength can be obtained from fibres contribution. Before it is built, a preliminary analysis considering all four Levels of Approximation is performed in order to evaluate the minimum shear reinforcement ratio and stirrups spacing to be inserted in the real structure. This procedure is suggested to be performed not only because the casting process affects the fibres dispersion and orientation, as previously explained, but the reinforcement ratio also affects the concrete flow. Since performing this preliminary analysis offers almost no logistics and costs compared to the mock-up construction approach, it can be seen as a starting point when designing any type of structural element which fibres dispersion and orientation for this specific type is not known.

Firstly, due to the complexity and novelty of these Levels of Approximation, an initial study considering reinforced concrete is presented. In parallel, NLFE models were developed and their strengths were compared.

At the end, considering the full understanding and validation of both analytical and nonlinear numerical model approaches the shear strength for a High Performance Fibre Reinforced Concrete is presented.

4.1 Levels of Approximation Curves for Reinforced Concrete

The behaviour of reinforced concrete beams is studied in terms of the characteristic shear stress, τ_R, defined as:

$$\tau_R = \frac{V_R}{b_w \cdot z} \tag{20}$$

Figure 6 shows the variation of τ_R obtained with all 3 Levels of Approximation for increasing transverse reinforcement ratio for a beam with the following characteristics: f_{ck} = 60MPa, f_{ywk} = 500 MPa, vertical stirrups, $\varepsilon_x = 0.001$. For low values of the reinforcement ratio the shear resistance is ruled by the yielding of the stirrups considering minimum angle θ until the maximum value of τ_R is reached for this angle. For the adopted value of ε_x, the minimum value for θ is 30º for all LoA and therefore the lines are parallel. For LoA III the contribution of the concrete is seen to increase the resistance for low reinforcement ratios.

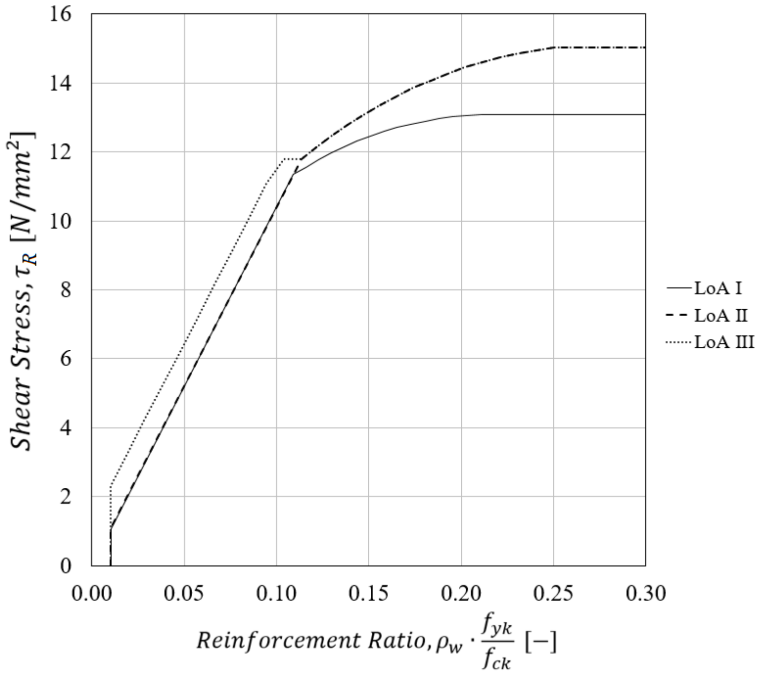

Figure 6. Levels of Approximation I to III for a 60N/mm² compressive strength concrete

For higher values of reinforcement ratio, the inclination of the compressive stress field, θ, that limits the shear strength by concrete crushing, may be calculated by equating Eqs. 3 and 5, yielding to, for reinforced concrete (RC):

$$sin\theta = \sqrt{\frac{\rho_z \cdot f_{yk}}{k_c \cdot f_{ck}}} \tag{21}$$

The results for θ are depicted in Fig. 7 where it can be seen the variation between θ_{min} and θ_{max}.

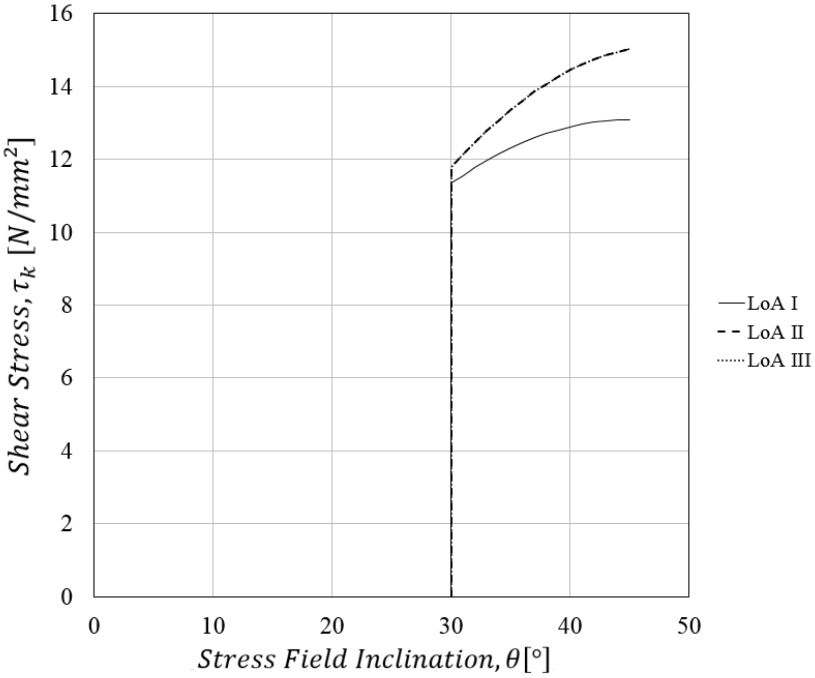

Figure 7. Variation of stress field inclination

4.2 Levels of Approximation Curves for HPFRC

In the case of HPFRC the angle q that limits the shear strength (by concrete crushing) is given by

$$sin\theta = \sqrt{\frac{\rho_z \cdot f_{yk} + k_f \cdot f_{Ftuk}}{k_c \cdot f_{ck}}} \tag{22}$$

A HPFRC with mean value of compressive strength equals to $f_{cm} = 68N/mm^2$ ($f_{ck} = 60N/mm^2$) developed at LabEST – Laboratory of Structures and Materials from COPPE-Federal University of Rio de Janeiro – was chosen (Marangon, 2011). A direct tensile test was performed on a 50mm-thick dogbone specimen (Fig. 8-a) and its tensile behaviour is plotted in Fig. 8-b.

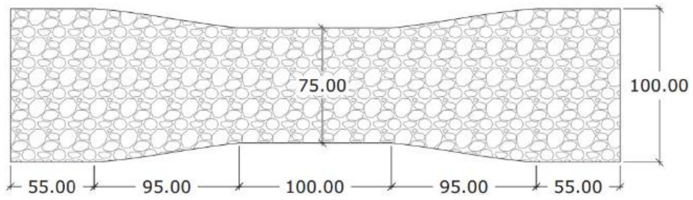

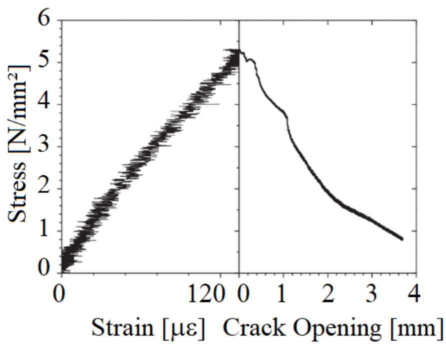

(a) **(b)**

Figure 8. Direct tensile stress of a HPFRC: (a) specimen and (b) tensile behaviour

Is must be emphasized that it is in Fig. 8-b where the problem lies. The tensile parameters (fracture energy, elastic tensile strength, post-cracking behaviour curve, etc.) used in Levels of Approximation, as well as FE models, are based on tensile test results. However, when building a new structure, the casting process and the formwork shape will be different than the specimen's, directly interfering in fibre dispersion and orientation. Therefore, every calculation in this paper is considered as preliminary until a mock-up is cast and the constitutive equations for each part of the structure can be obtained.

Being that, the shear stress curves taking into account the contribution of steel fibres are obtained from the following parameters, taking into account the same value for longitudinal strain at mid-depth, $\varepsilon_x = 0.001$:

$$\theta_{min} = 36°$$

$$w_u = 1.2mm$$

It must be emphasized that when steel fibres are added to the cementitious matrix, a different equation for stress field inclination is provided (Eq. 18). Thus, under the same flexural and shear stresses, a minimum inclination is given for each type of material, RC ($\theta_{min} = 30°$) and HPFRC ($\theta_{min} = 36°$). For crack opening, w_u, its respective stress is taken from Fig. 8-b as $f_{Ftuk} = 3.18N/mm^2$. Thus, the contribution to shear strength attributed to the steel fibres is

$$\tau_{fibres} = 0.8 \cdot 3.18 \cdot \frac{1}{tan36°}$$

$$\tau_{fibres} = 3.50N/mm^2$$

Figure 9 shows the Levels of Approximation when considering steel fibres addition.

Proceedings of the XXXVIII Iberian Latin-American Congress on Computational Methods in Engineering
P.O. Faria, R.H. Lopez, L.F.F. Miguel, W.J.S. Gomes, M. Noronha (Editores), ABMEC, Florianópolis, SC, Brazil, November 5-8, 2017.

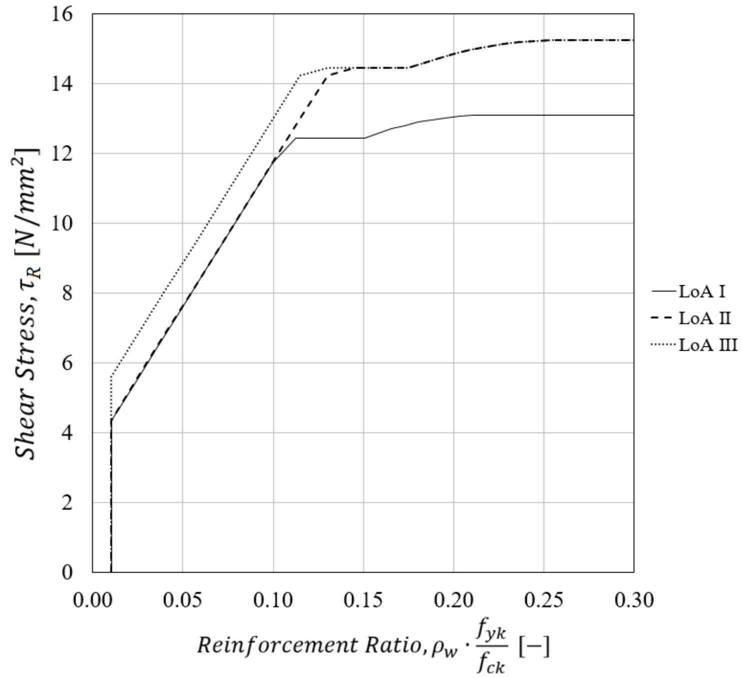

Figure 9. Levels of Approximation I to III for RC and HPFRC

4.3 Proposed Geometry for FE Analyses

In order to perform FE analyses, the proposed geometry is presented in Figure 10. The depth to span ratio was successfully tested in beams experiments by Hao & Ning (2012).

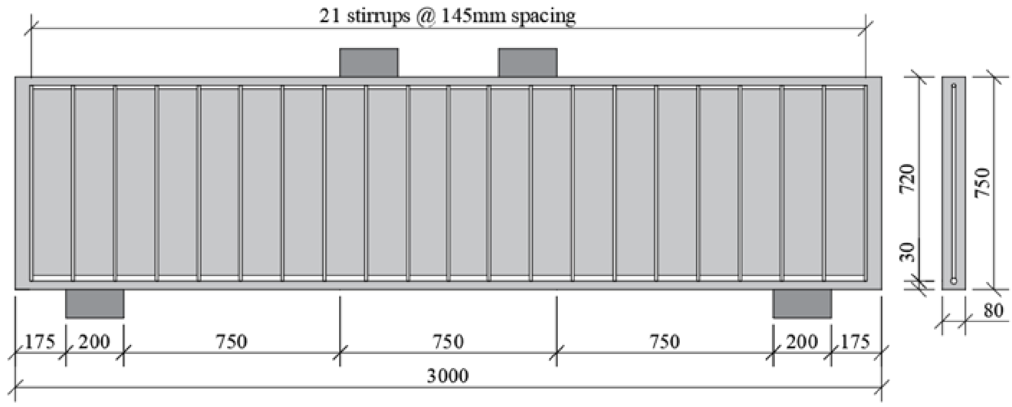

Figure 10. Proposed beam cross-section and its passive reinforcements (units in mm)

4.4 Finite Element Model's input data

All tests were modelled in the Finite Element Method software DIANA© FEA 10.1. For that, 2-D modelling was applied considering the Multi-Directional Fixed Crack Model due to its unknown fracture plane. The 12.5 x 12.5 mm² bi-dimensional elements were generated by a quadrilateral mesher type, with quadratic mesh order and linear interpolation at each mid-side node location (Fig. 11).

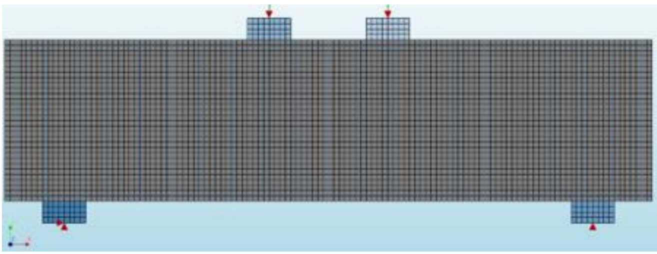

Figure 11. FE model mesh: 12.5x12.5 mm² quadrilateral elements

For the reinforced concrete models, a linear softening curve based on Fracture Energy, G_f, was chosen, as it presented good behaviour for shear analysis (Araújo et al, 2010). Fracture Energy, Young Modulus and Tensile Strength parameters were obtained from *fib* Model Code 2010 (fib, 2012) equations, respectively:

$$G_F = 73 \cdot f_{cm}^{0.18} \tag{23}$$

$$E_{ci} = 21500 \cdot \left(\frac{f_{ck} + 8}{10}\right)^{\frac{1}{3}} \tag{24}$$

$$f_{ctk,0.05} = 0.21 \cdot f_{ck}^{\frac{2}{3}} \tag{25}$$

Mohr-Coulomb was adopted as material's plasticity criterion – its parameters (Cohesion, Friction angle, Dilatancy angle, Friction Hardening type and Tension cut-off) were obtained based on DIANA user's manual, edited by Manie & Kikstra (2016-a, 2016-b). When considering steel fibre contribution, a multi-linear softening curve was selected and values from Fig. 8-b were adapted to be as in Fig. 12.

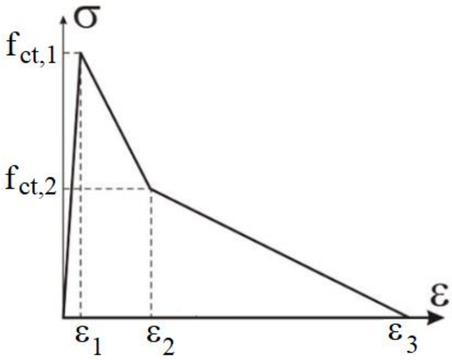

Figure 12. Typical Stress-Strain Curve for Fibre Reinforced Concrete

Two types of steel were considered: the first type, for the supporting and loading plates, presented elastic behaviour, Young Modulus E_s = 210,000 N/mm² and Poisson Coefficient ν = 0.3 as only parameters. The second, adopted for every reinforcement bars in the model, considered the same numerical parameters as in the first, plus yield stress f_y = 500N/mm², an ultimate tensile strain of $\varepsilon_{su,t}$ = 0.01 and an ultimate compressive strain of $\varepsilon_{su,c}$ = 0.0035. In addition, the reinforcement type was refined as embedded. For both types of concrete, RC and HPFRC, compressive strength was equals to 60N/mm², accordingly to test results performed by Marangon (2011).

The applied load was selected to be displacement loading, with 0.25mm at each step. The chosen iterative method was Secant (Quasi-Newton) with Crisfield algorithm type, combined with Line Search Method, which enhances the convergence (Bettin, 2013). The convergence norm was based in energy with a convergence tolerance of 2.5 x 10^{-4}.

4.5 Shear Strength Values from the Levels of Approximation and FE Models

To compare the analytical results of the three Levels of Approximation to the finite element models outputs, two transverse reinforcement ratios were selected and their respective shear stress were obtained. From Fig. 7 and Fig. 9, the shear stresses were obtained from reinforcement ratios, $\rho_z \cdot \frac{f_{yk}}{f_{ck}}$, being equal to 0.05 and 0.10 (Table 1).

Table 1. Analytical Results and Numerical Outputs

Material	f_{ck}	θ_{min} [°]	$\rho_w \cdot \frac{f_{yk}}{f_{ck}}$	V_{LoA} $[kN]$			DIANA©	
				I	II	III	V_y $[kN]$	V_u $[kN]$
RC	60	30	0.05	269	269	333	367	367
			0.10	539	539	603	506	617
HPFRC	60	36	0.05	395	395	549	619	687
			0.10	609	609	674	747	839

Note:
V_y = Shear loading when first stirrup started yielding process
V_u = Ultimate shear loading

Independently of the considered ratios the failure mode observed in all FE models were transverse reinforcement yielding type (specifically all stirrups between loading plate and supporting plate yielded), since no flexural failure was observed nor web crushing were registered.

From Table 1 it is possible to notice that all three Levels of Approximation provide satisfactory results when comparing to the finite element model's outputs, being Level III the most accurate amongst the analytical solutions, as stated before. Although considered to be the simplest approach, Level of Approximation I provided satisfactory results and can be easily recommended when in preliminary design stage. Being all analytical models based on the equilibrium of forces of a truss model, a comparison amongst their values with DIANA's shear loading at yielding process is found reasonable; the difference amongst analytical and numerical values is up to 19%. On the other hand, since DIANA's analyses provides crack propagation, an ultimate shear loading can be provided, taking into account a more realistic behaviour. Considering that, LoA's results differ from numerical outputs up to 43% (LoA I and II) and 20% for LoA III.

Figures 13 to 15 illustrate, respectively, Principal Stresses S1 (compressive), Principal Stresses S2 (tensile) and Crack Pattern, between the two types of materials, being the RC-type modelled with linear softening curve model and the other, HPFRC-type, with multi-linear softening curve model. Firstly, as the beams have a different transverse reinforcement ratio and softening curves, hence different mechanical behaviour, the loadsteps performed in the analyses were different. Therefore, each evolution shown in Figure 13 to 15 illustrates the initial step, 25%, 50%, 75% of the analyses, and the final step.

Figure 13 shows the evolution of Principal Stress S1 (tensile stress) whereas it is possible to notice the contribution of steel fibres when under tensile stress. Withstanding 5.22N/mm², 64% greater than RC type, the last steps for HPFRC beams depicted in Fig.16-e and -f show similar stress distribution to 50% of steps for RC (Fig.16-b and -c), stating that steel fibres contribute to an evenly tensile stress distribution due to its bridge effect (Bentur & Midess, 2007). Also, between each material type it is possible to notice a smooth stress distribution when low transverse reinforcement is used.

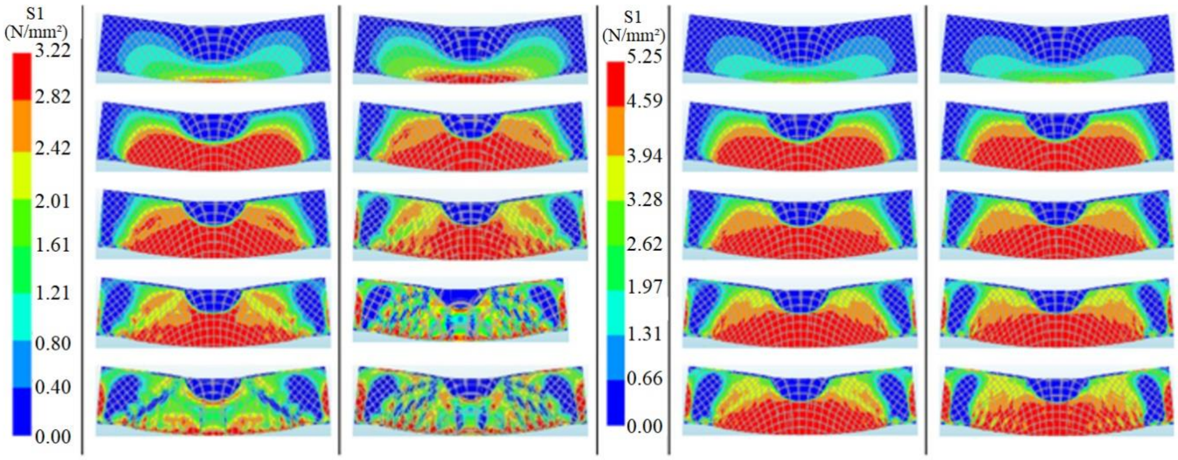

(a) (b) (c) (d) (e) (f)

Figure 13. Principal Stress S1 (Tensile Stress) in the concrete for f_{ck} = 60N/mm²: (a) RC tensile strength range, (b) RC with $\rho = 0.0060$ and (c) with $\rho = 0.0120$, (d) HPFRC tensile strength range, (c) HPFRC with $\rho = 0.0060$ and (f) with $\rho = 0.0120$

Figure 14 shows the evolution of Principal Stress S2 (compressive stress) whereas it is possible to notice that the contribution of steel fibres increases shear strength. Although ultimate compressive strength is rarely altered by fibre addition (Bentur & Midess, 2007), and as long as web crush limit is not reached, steel fibres addition behaves as extra reinforcement, allowing shear strength to increase. Adding up to 2% of steel fibre in volume can increase up to 100% in shear strength (Araújo et al, 2010). Thus, it is possible to notice the increase of compressive stress distribution as shear reinforcement increases and RC is changed to HPFRC. Although Fig. 14-e shows the most intense compressive stress distribution compared to the other three models, no web crushing was registered during the simulations. A web crush scenario would be detected if a uniform colour depicting 60N/mm² would diagonally cross from supporting plate to loading plate.

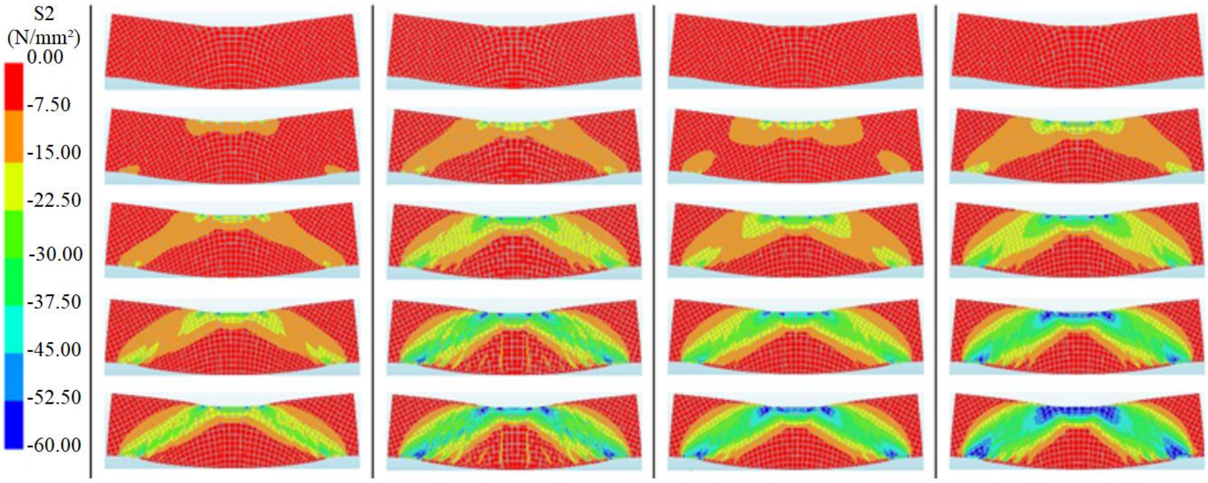

(a) (b) (c) (d) (e)

Figure 14. Principal Stress S2 (Compressive Stress) in the concrete for f_{ck} = 60N/mm²: (a) RC compressive strength range, (b) RC with $\rho = 0.0060$ and (c) with $\rho = 0.0120$, (d) HPFRC with $\rho = 0.0060$ and (f) with $\rho = 0.0120$

Figure 15 shows the evolution of Crack Pattern. As expected for a *deflection hardening* material, steel fibres enhance cracking behaviour due to its bridge effect and positively affect the durability of the material (Bentur & Midess, 2007) turning a single localised macro crack into multiple dispersed micro cracks. As it can be seen, for considerable greater loads (as shown in Table 1), crack pattern from HPFRC beams show a smoother crack distribution.

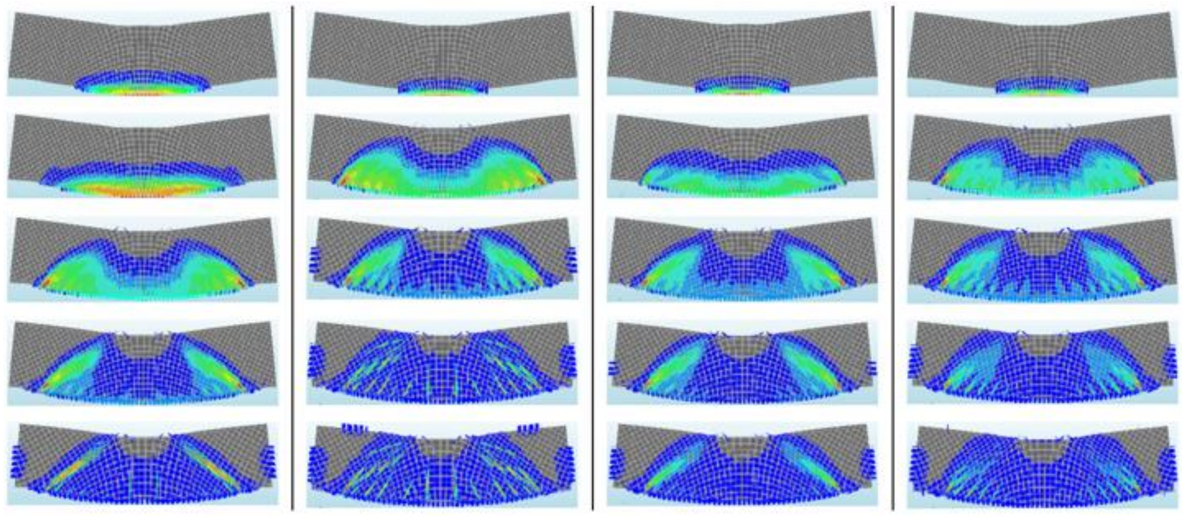

(a) (b) (c) (d)

Figure 15. Crack pattern in the concrete for f_{ck} = 60N/mm²: (a) RC with $\rho = 0.0060$ and (b) with $\rho = 0.0120$, (c) HPFRC with $\rho = 0.0060$ and (d) with $\rho = 0.0120$

5 CONCLUSIONS

From the three analytical methods, being Level of Approximation I the simplest, and Level of Approximation III the most complex amongst analytical solutions, shear strength for RC increased up to 24% as accuracy increased for low transverse reinforcement ratio and up to 12% for high transverse reinforcement, whilst respectively 38% and 11% were observed for HPFRC.

A comparison between each LoA's RC result and its respective FE model showed that satisfactory results can be obtained from analytical results. A satisfactory convergence for all results for Level of Approximation III was observed when comparing to FE outputs.

In general, the outputs obtained from NLFEA proved to be greater than the analytical results obtained with the most complex Level of Approximation, III. Although NLFEA is a powerful tool for predicting structure's mechanical behaviour, the model outputs are heavily dependent on the modelling choices, such as element type, constitutive and crack models, as well as convergence parameters, etc. In opposition to calculation procedures provided by design codes, there is no strict guidance on how to create a model of a structure using a finite element analysis tool. Therefore, scattered outputs are still expected amongst different approaches for numerical models developed by structural engineers.

Finally, the investigation of the Levels of Approximation compared to the FE models shows that, not only the initial exposed problem of fibre dispersion must be experimented in laboratory, but also shear strength tests must be performed. With these experimental tests, it will be possible to validate and calibrate all FE models presented in this paper.

ACKNOWLEDGEMENTS

The authors would like to thank CAPES and CNPq for the financial support.

REFERENCES

Araújo, D. L., Carmo, L. C., Nunes, F. G. T, Toledo Filho, R. D., 2010. Computational modeling of steel fiber reinforced concrete beams subjected to shear. *IBRACON Structures and Materials Journal*, vol 3, n 1, pp. 68 – 94. IBRACON.

ASCE-ACI Task Committee 426, 1973. The Shear Strength of Reinforced Concrete Members. Journal of the Structural Division, Issue 6, pp 1091-1187.

Association Française de Génie Civil (AFGC) & Service d'Étude des Transports, des Routes et de leurs Aménagement (SETRA), 2013. *Ultra High Performance Fibre-Reinforeced – Recommendations*.

Belletti, B., Damoni, C., den Uijl, J. A., Hendriks, M. A. N., Walraven, J. C., 2013. Shear Resistance Evaluation of Prestressed Concrete Beams: fib Model Code 2010 guidelines for Level IV Approximations. *Structural Concrete*, vol 14, n 3, pp. 242-249. Wiley-*fib*.

Bentur, A., Mindess, S., 2007. *Fibre Reinforced Cementitious Composites*. 2nd Edition. Taylor & Francis.

Bentz, E. C., 2010. MC2010: Shear Strength of beams and implications of the new approaches. *Shear and Punching Shear in RC and FRC*, *fib* Bulletin 57. Lausanne, Switzerland.

Bettin, W. P., 2013. *Modelagem de Lajes Alveolares com a Utilização de Concreto com Fibras Metálicas e Cinza do Bagaço de Cana-de-Açúcar*. Master thesis, Federal University of Rio de Janeiro, Brazil.

Fedération Internationale du Béton (*fib*), 2012. *Model Code 2010 – final draft*, vol. 1, Bulletin 65, and vol. 2, Bulletin 66, Lausanne, Switzerland.

Hao, D., Ning, C., 2012. Detailed Study of the Cracking Process at Shear Failure through FE Analysis of Beam Experiments. Master thesis, Chalmers University of Technology, Sweden.

Lantsoght, E., de Boer, A., van der Veen, C., 2017. Levels of approximation for the shear assessment of reinforced concrete slab bridges. *Structural Concrete*, vol 18, n 1, pp. 143-152. Wiley-*fib*.

Manie, J., Kikstra, W. P., 2016. *DIANA User's Manual – Material Library – Release 10.1*. DIANA FEA BV.

Manie, J., Kikstra, W. P., 2016. *DIANA User's Manual – Analysis Procedures – Release 10.1*. DIANA FEA BV.

Marangon, E. 2011. *Caracterização Material e Estrutural de Concretos Autoadensáveis Reforçados com Fibras de Aço*. PhD thesis, Federal University of Rio de Janeiro, Brazil.

SFRC – Consortium, 2013. *Guideline for execution of steel fibre reinforced SCC*, Danish Technological Institute, Taastrup, Denmark.

Sigrist, V., Bentz, E., Ruiz, M. F., Foster, S., Muttoni, A., 2013. Background to the *fib* Model Code 2010 shear provisions – part I: beams and slabs. *Structural Concrete*, vol 14, n 3, pp. 195-203. Wiley-*fib*.

Sigrist, V. & Hackbarth, B., 2010. A Structured Approach to the Design and Analysis of Beams in Shear. *Shear and Punching Shear in RC and FRC*, *fib* Bulletin 57. Lausanne, Switzerland.

Sigrist, V. & Hackbarth, B., 2012. Design and Analysis of Members in Shear. *Design of Concrete Structures Using Eurocodes – Third International Workshop*.

Sorelli, L. G., Ulm, F. -J, Toutlemonde, F., 2007. Fracture Stability and Micromechanics of Strain Hardening Cementitious Composites. *6th Int. Conf. on FRActure Mechanics of Concrete and Structure (FRAMCOS)*, pp. 1403-1412.

Svec, O., Thrane, L. N., Stang, H., 2014. Linking the Fibre Orientation Factor with the Mechanical Response of the fibre reinforced Self-compacting Concrete. *Nordic Concrete Research*, vol 49, pp. 17-26.

Walraven, J. C., 2009. High Performance Fibre Reinforced Concrete: Progress in Knowledge and Design Codes. *Materials and Structures*, vol 42, pp. 1247-1260.